DOI: 10.3969/j.issn.1673-5188.2018.01.003
http://kns.cnki.net/kcms/detail/34.1294.TN.201800319.1042.002.html, published online March 19, 2018

Design of Wireless Energy-Harvested UHF WSN Tag for Cellular IoT

LI Gang, XU Rui, LI Zhenbing, ZHOU Jie, LI Jian, and WEN Guangjun
(Centre for RFIC and System, School of Information and Communication Engineering, University of Electronic Science and Technology of China, Chengdu 611731, China)

Abstract

In this paper, a wireless energy-harvested ultra-high frequency (UHF) wireless sensor network (WSN) tag is designed and implemented for cellular IoT applications. The WSN tag is made up of a wireless energy harvesting circuit, a temperature sensing circuit, and a radio frequency identification (RFID) tag. The developed WSN tag is compatible with the ISO/IEC18000-6C protocol. The WSN tag can receive the GSM RF energy operating in China GSM900 and GSM1800 bands in the surrounding environment and the solar energy, then converts the RF energy to direct current (DC) by schottky diode-based rectifying circuit, and finally stores the DC energy in a supercapacitor through a DC-DC booster circuit. The DC-DC booster circuit drives the front-end circuit, TI MSP430 microcontroller, temperature sensing circuit, and other active circuits in the tag. The MSP430 works in low-power mode when it is powered up, and it can also reduce power consumption more by reducing main clock (MCLK) frequency according to different forward link rates. The implemented WSN tag demonstrated that the RF-to-DC conversion efficiency is higher than 39% when the receiving 900 MHz RF signal power is from -14 dBm to 0 dBm and could make the tag work normally. The signal receiving sensitivity of the WSN tag is up to -32 dBm at the rate of 40 kbit/s from the Reader to the WSN tag. The WSN tag supports Miller coding and extended Miller coding. This wireless energy harvested UHF WSN tag, compared with conventional UHF passive tags and battery-powered active UHF RFID Tags, has many advantages, such as far communication distance, long service life, and sensing functionality. It will have wide applications in the Internet of Things (IoT).

Keywords

DC-DC booster circuit; MSP430; RF energy harvest; WSN tag

1 Introduction

Radio frequency identification (RFID) is a well-known non-contact automatic identification technology widely used in identification, supply chain, logistics, retail, manufacturing, garment industry, medical industry, identity and anti-counterfeiting and many other related applications [1]. RFID tags can be classified as passive tags, active tags and semi-active tags. The passive tags gain the power from reader emitting out RF signal in the near distance, so it has no DC power supply [2]. Active tags have their own DC energy source and can transmit actively signal; therefore they have better performance than passive tags. Semi-active tags extract the power from their battery, and have a large operating distance.

In traditional wireless sensor network, almost all the wireless sensing nodes (it is also called as wireless sensing tags) operate in active mode or semi-active mode, they get the energy come from the rechargeable battery or other power supply. However, the rechargeable battery has the disadvantages of frequent maintenance and the limited number of charge cycles. For the advantage of battery-free operation, low-cost passive sensing tags have got much attention. A convenient solution is to provide energy for the sensing tags by harvesting ambient RF energy sources [3]. The RF energy from the environment can greatly extend the life of wireless sensor networks (WSN) [4]. The ambient RF energy is a type of new energy everywhere. Sustainability makes ambient RF energy more reliable than other types of new energy, such as solar energy and wind energy.

This work was supported in part by Guangdong Provincial Science and Technology Planning Program (Industrial High-Tech Field) of China under project contracts No. 2016A010101036, and in part by Sichuan Provincial Science and Technology Planning Program (Technology Supporting Plan) of China under project contracts No. 2016GZ0061 and No. 2016GZ0116 and No. 2017GZ0336, in part by the fundamental research funds for the Central Universities under project contract No. ZYGX2016Z011, and in part by the National Natural Science Foundation of China under project contracts No. 61371047, No. 61601093 and No. 61701082.

Many studies have been reported on energy harvesting systems operating on a single band or dual bands. The proposed techniques involve a quad-band energy harvester [5], a dual-band integrated wireless energy harvesting system [6], a rectenna operating in the GSM band [7], and a RF power harvesting system operating in GSM900 and Wi-Fi 2.45 GHz bands [8]. These techniques may be adopted to develop new battery-free wireless sensing tags and WSN. Herein, in this paper, a wireless energy-harvested ultra-high frequency (UHF) WSN tag is proposed. The WSN tag is designed to be implemented by the use of commercial discrete components, on PCB board, instead of conventional RFID ICs. The advantages of PCB design over IC design are fast design iteration time, low development cost and quickly changing the design according to the designer's intentions [9].

This paper is organized as follows. Section 2 describes the WSN tag system architecture. Section 3 details the WSN tag implementation, including the design method of tag circuits and the protocol programing procedure. Section 4 tests the WSN tag. Finally, Section 5 concludes this WSN tag design.

2 WSN Tag System Architecture

Fig. 1 shows the system structure of the proposed wireless energy-harvested UHF WSN tag. Here, the system architecture including the rectifying circuit, power manager, modulator, demodulator, sensor and baseband signal processor is described in detail below.

The rectifying circuit harvests RF energy from GSM900 and GSM1800 bands in China and is divided into two rectifier branches utilizing a diplexer, which has high pass and low pass filter functions. The RF-to-DC conversion efficiency is in the range of 20%−63.2% while the input power is in the range of −22 dBm to 1 dBm in GSM900 band, and in the range of 13.8%−55.5% while the input power is in the range of −22 dBm to 3 dBm in GSM1800 band. The solar panel collects solar energy and directly connects the output to the DC booster.

The cold start voltage of the direct current (DC) booster, regulator and power manager circuit is 330 mV [10]. The DC booster circuit harvests energy from the rectifier circuit, charges the supercapacitor, and stops to charge when the voltage is up to the threshold. The threshold can be determined by setting the external resistors of the DC booster chip.

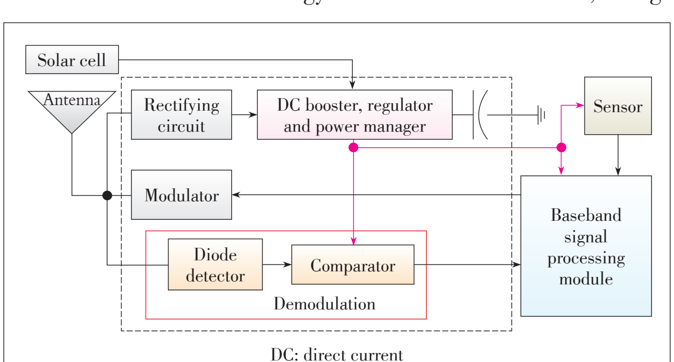

▲Figure 1. The proposed wireless energy-harvesting UHF WSN tag scheme.

The modulator controls the state of impedance matching by using gate-controlled metal oxide semiconductor (MOS). The microcontroller unit (MCU) outputs low level signal to make the impedance match and outputs high level signal to make the impedance mismatch. The WSN tag backscatters the RF signal to the reader, and the reader determines whether the reply signal of the tag is high or low according to the reflecting RF energy. The demodulator circuit consists of a diode detector and a comparator. The demodulation circuit uses the Schottky diode. The comparator uses the low voltage comparator chip.

The baseband signal processor implements the ISO/IEC 18000-6C protocol standard, and the detailed design process is described in section 3. The temperature sensor is used to detect temperature in the ambient environment. The temperature sensor can operate at a supply voltage as low as 1.5 V, while operating over the wide temperature range of −50 °C to +150 °C. The temperature sensor delivers an output voltage that is inversely proportional to the measured temperature, and its low supply current makes it ideal for battery-powered systems as well as general temperature sensing applications [11]. In the WSN tag, the gain selects (GS) of the temperature sensor are both set to zero, so the voltage output can be approximately expressed as follows.

$$V = (-5.50\ \mathrm{mV}/^{\circ}C) \times T + 1035\ \mathrm{mV}. \qquad (1)$$

3 WSN Tag Implementation

In this paper, the onboard MSP430FR5969 microcontroller is responsible to achieve a WSN Tag [12]. The MCU has ultra-low power consumption features, which is widely used in the pre-research of low-power systems. The WSN tag achieves the ISO/IEC18000-6C protocol standard and can be identified by Impinj R420 reader.

The most difficult aspect of a WSN tag is to meet the timing requirement and reduce the power consumption at the same time. It is essential to have a high efficient programming method for the low power requirements. The proposed system reduces MCLK and operates alternately between the low power mode and the active mode to improve the tag performance. The WSN tag supports all the mandatory commands specified in the ISO/IEC 18000-6C protocol and adds a low speed mode (less than 40 kbit/s) to the general ISO/IEC18000-6C protocol. Simultaneously, the WSN tag extends Miller coding function [13]. The low-speed mode is used to reduce power consumption, so that the main clock operating frequency is lower. The extended miller subcarriers can reduce interference. The WSN tag protocol implementation flow chart is shown in **Fig. 2**.

In the RX_IN module in Fig. 2, the delimiter of input signal from the reader needs be detected, and the delimiter is at a low

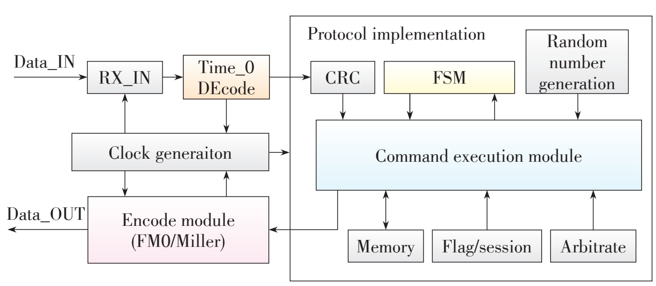

CRC: cyclic redundancy check FSM: finite state machine

▲Figure 2. MCU achieving RFID tag protocol.

level and kept about 12.5 μs. The MCU will execute Timer_0 module when the active delimiter is detected. The Timer_0 module achieves decoding function by timer interrupt, and the MCU will start working according to the command received. The Timer_0 module is configured as a rising edge trigger to receive the input signal. The MCU will trigger the interrupt when the rising edge is detected. The interrupt routine uses the current counter value minus the value of the previous counter value to indicate the time interval between two input signals at the rising edge. In the Timer_0 interrupt routine, the time interval of two adjacent rising edges will be frequently used to determine the level of input data. The Timer_0 module decodes the forward link data, extracts the forward link rate and Rtcal/Trcal length, and provides the relevant data for the execution module. If the downlink link rate is lower than 40 kbit/s, the MCLK frequency of the MCU can be set to lower for reducing power consumption according to the length of data0.

The command execution module implements all the other functions of the WSN tag, including cyclic redundancy check (CRC), finite state machine (FSM) implementation, random number generation, arbitration module, command processing, interrupt control, timing control, working mode switching, and so on. In this paper, the sensing command of detecting the ambient temperature and humidity has been implemented. The sensing functions are very important for a WSN tag; the tag collects various sensing information and replies the information to the reader, which may analyze the sensing information to get the specific environment information.

The random number generation module generates the 16 bits pseudo-random number for the communication reliability between tags and readers. The CRC16 of the {PC+ XPC + UII} calculates at power-up which is used as the seed of the pseudo-random number. The {PC+ XPC + UII} varies in different tags, so the seeds are different too. The pseudo-random number generation algorithm also provides the pseudo-random number for the handling signal. The encoding module encodes and transmits reply data. The MCU can configure a variety of clock frequency to support the different backscatter link frequency by calling the clock generation module. At the same time, the WSN tag supports the forward and backscatter rates less than 40 kbit/s and also supports extension miller subcarrier (the Miller sequence would contain exactly 2, 4, 8, 16, 32, 64, 128 or 256 subcarrier cycles per bit). The clock generation module may set the MCU clock cycles. The highest master clock frequency, MCLK, is 16 MHz. The MCU can quickly change its MCLK frequency through its registers base on the backscatter-link frequency (BLF) parameter.

3.1 Sensing Function

The custom sensing command is used to collect almost all sensory information, including temperature information, humidity information, pressure information, and other information. **Table 1** shows the formats of the custom sensing commands and **Table 2** shows its reply formats.

The command field is defined as 0xE001. The WSN field is a parameter of the custom sensing command, and its value represents the type of sensing information. That the WSN is 1 indicates the tag will collect temperature information, and that the WSN is 2 indicates the tag will collect humidity information.

The WrEn field indicates whether the WSN tag collects the sensing information or not, and whether it writes the information collected to memory or not. If WrEn is 2’b00, it indicates that the WSN tag does not collect sensing information, reads the sensing information base on the address of the WSN tag distribution and returns sensing information to the reader. If WrEn is 2’b01, it indicates that the WSN tag does not collect sensing information, reads the sensing information base on the address of the wordPtr field and returns sensing information to the reader. If WrEn is 2’b10, it indicates that the WSN tag collects the sensing information, writes the sensing information to the assigned address by the WSN tag and returns the information to the reader. When WrEn is 2’b11, it indicates that the WSN tag collects the sensing information, writes the sensing information to the address of WordPtr field and returns the sens-

▼Table 1. The sensor command formats

	Bits	Description
Command	16	0xE001
WSN	16	0=RFU, 1=temperature, 2=humidity
RFU	16	0x0
WrEn	2	00=fix read, 01=read 10=fix write, 11=write
WordPtr	8	Word address pointer
RN16	16	Handle
CRC16	16	Checksum

▼Table 2. Tag replies to the sensor commands

	Header	WSN Data	RN16	CRC16
Bits	1	16	16	16
Description	0	Data	Handle	Checksum

ing information to the reader.

The WordPtr field indicates the address where the WSN tag writes the information collected to the memory. RN16 field is a 16-bit tag-authentication number. CRC16 field is the CRC check code for ensuring communication reliability. The custom sensing command has a total of 90 bits. The sensing information collected directly by the sensor connects to the analog to digital converter (ADC) of the MCU through analog input pin (the different sensing functions connect different input pins). ADC converts the input analog signal into the digital output (N_{ADC}) and stores N_{ADC} in the corresponding registers. The ADC supports 12-bit analog-to-digital conversion, and the ADC conversion formulas for N_{ADC} are shown as follows.

$$N_{ADC} = 4096 \times \frac{(V_{in+} + \frac{1}{2}LSB) - V_{R-}}{V_{R+} - V_{R-}}, \quad (2)$$

$$1LSB = \frac{V_{R+} - V_{R-}}{4096}. \quad (3)$$

Fig. 3 shows the execution of the custom sensing command. When receiving the sensing command, the MCU will jump to the subroutine and then verify the CRC-16 and 16-bit tag-authentication number (handle). If the CRC-16 and handle both pass the validation, the MCU will continue to execute this subroutine, otherwise it will terminate the process directly. The WSN field is used to select different functions of the wireless sensor network. The WrEn is used to select reading and writing. Finally, if the WSN tag passes the validation, it replies to the custom sensing command (Table 2), otherwise the WSN tag remains silent.

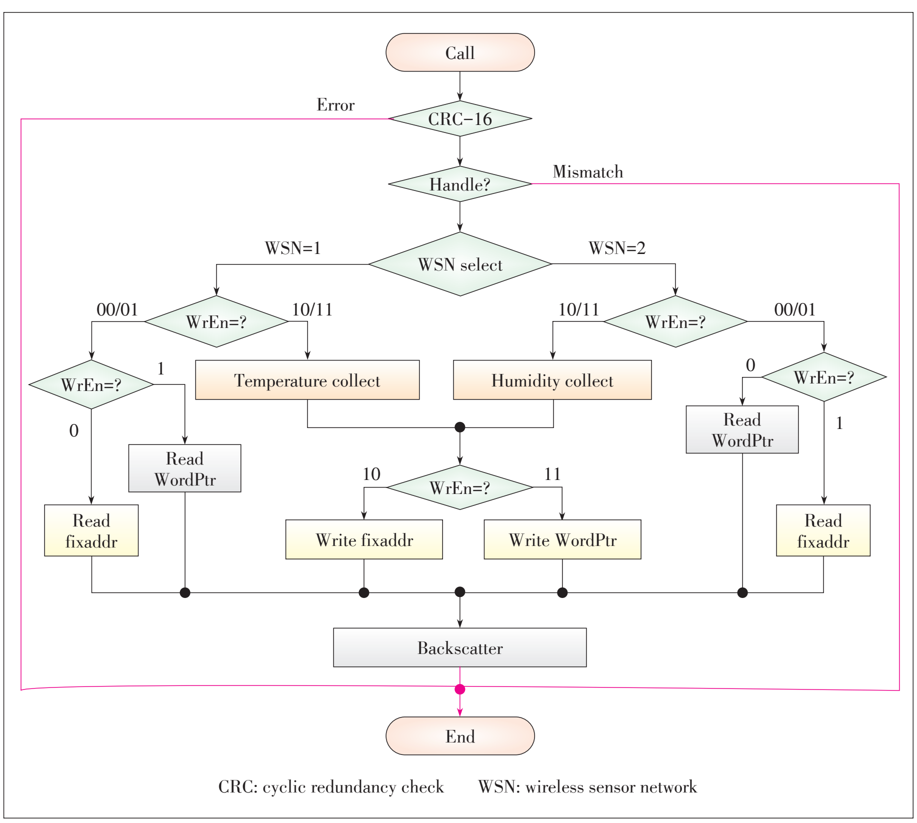

▲Figure 3. The execution of the sensing command.

3.2 Miller Coding

The MCU realizes miller coding to meet the ISO/IEC18000-6C protocol standard. The miller coding rules are defined as follows. The original symbol "1" does not convert at the beginning and conducts conversion at the center point. The original symbol "0" is divided into a single "0" or a continuous "0" to be treated differently. When a single "0" appears, the electrical level before 0 is unchanged, even if the electrical level does not convert at the symbol boundary and is meta-intermediate. For the continuous "0", the electrical level converts at the border of two consecutive "0".

Firstly, the program encodes the miller preamble according to the TRext value of Query commands. When TRext is 0, the program sends the number of four times M values square waves; when TRext is 1, the program sends the number of sixteen times M values square waves. Secondly, the program adds to a string of 0100111_b at the end of square waves. The miller coding uses the shortest instruction to meet the timing requirement, and the jump range of the JMP instruction must be fewer than 512 words to avoid using extra clock cycles for the instruction. The MCU must separate two subcarrier sequences from other subcarrier sequences, because the two subcarrier sequences have only two subcarriers which are not possible to encode all bits as other subcarrier sequences encoding with five clock cycles. The loop jump needs to determine the number of subcarriers and the jump needs two clock cycles, but the program must determine to send 1 or 0 level in five clock cycles. Thus, it is necessary to distinguish two subcarrier sequences from other subcarrier sequences for meeting the timing requirement.

The miller coding is shown in **Fig. 4**. When the main program jumps to the miller coding through a jump command, the program must first configure the specific output ports and specific MCLK according to the BLF. Then, the program jumps to M2 (two subcarriers) module when the M value specified in the Query command is one, otherwise it jumps to Mx (more subcarriers than two subcarriers) module. The TRext specified in the Query command determines the number of pilot tone sent. The program jumps to M_byte1_bit0 if the

D:\EMAG\2018-02-61/VOL16\F3.VFT——7PPS/P4 bits_cnt (bits_cnt is zero for the entire byte, vice versa) is zero, otherwise jumps to Send_byte1_bit1. Taking miller value 2 as an example, **Fig. 5** shows the encoded miller preamble.

The WSN tag expands the M values specified by the ISO/IEC18000-6C protocol standard, and the expanded M values shall be confirmed according to the custom command. For simplicity and compatibility, the target (Target = 101 and 110) of the select command is used to select different M values. The custom parameters are shown in **Table 3**.

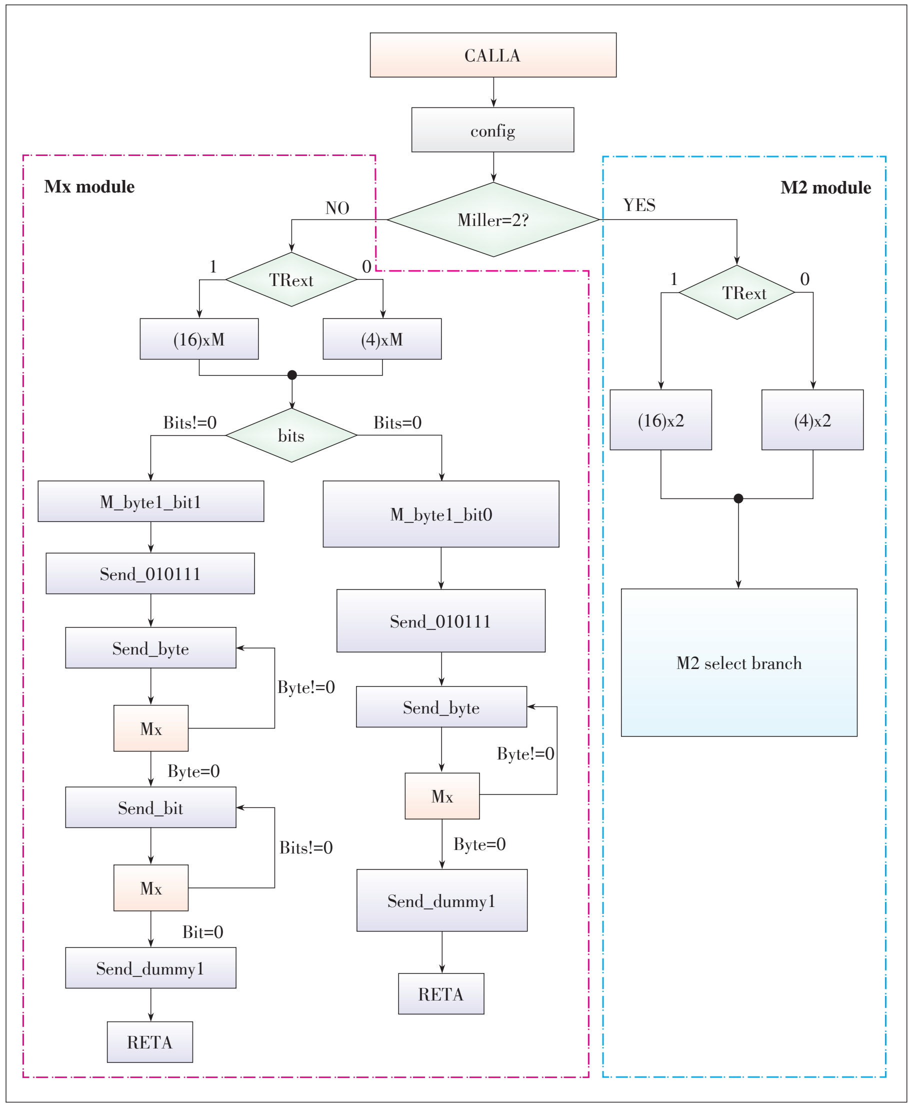

▲Figure 4. Miller coding.

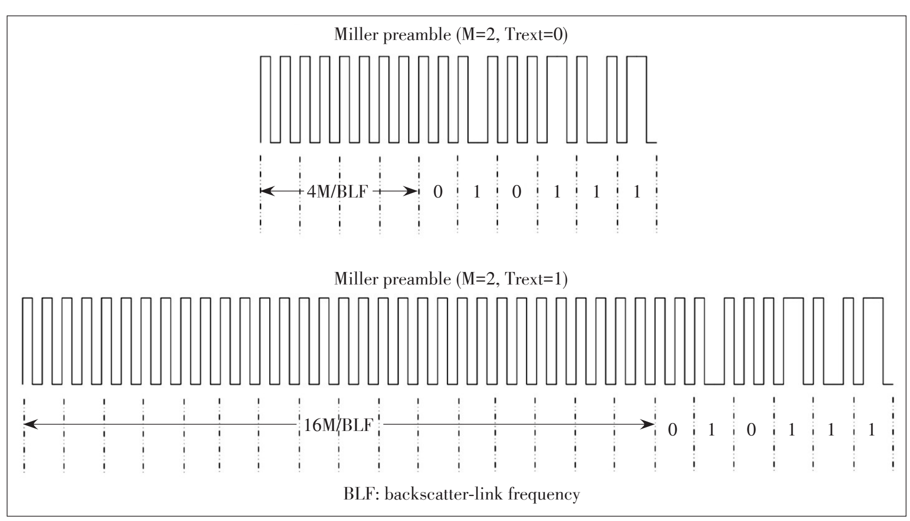

▲Figure 5. The encoded miller preamble (M=2).

4 Realization and Testing of Wireless Energy Harvest ER Ultra High Frequency IoT Tag

The proposed WSN tag was tested with a commercially available UHF RFID reader. The functions of the energy harvesting, ISO/IEC18000-6C protocol and temperature sensing were tested. The tested results are basically consistent with the theoretical analysis. The both front and back of the WSN tag circuit board are shown in **Fig. 6**.

4.1 Testing of Energy Harvesting

The WSN tag combines RF energy and solar energy for cellular IoT applications. The test of the energy harvesting performance was conducted in a wireless environment. The gain of transmitting antenna was 12 dBi, and the R420 reader provided 30 dBm transmit power. The gain of receiving antenna was 8 dBi. The two antennas kept 1 m away. The energy harvesting circuit can be charged in the wireless environment. The voltage of the super capacitor could reach 5.09 V within 24 s. The WSN tag can also turn solar energy into electricity by a solar panel, and the time of charging the supercapacitor up to 4.2 V is about 15 m.

4.2 Testing of Temperature Sensing

The temperature sensor was fixed to work in the mode which the gain selects are zero. The temperature sensing performance was tested in a high-low temperature test chamber from −30°C to 60°C with

▼Table 3. The compatibility table of the expanded M values

Target	M	Encode
3'bxxx	2'b00	FM0
3'b0xx	2'b01	M2
	2'b10	M4
	2'b11	M8
3'b101	2'b01	M16
	2'b10	M32
	2'b11	M64
3'b110	2'b01	M128
	2'b10	M256

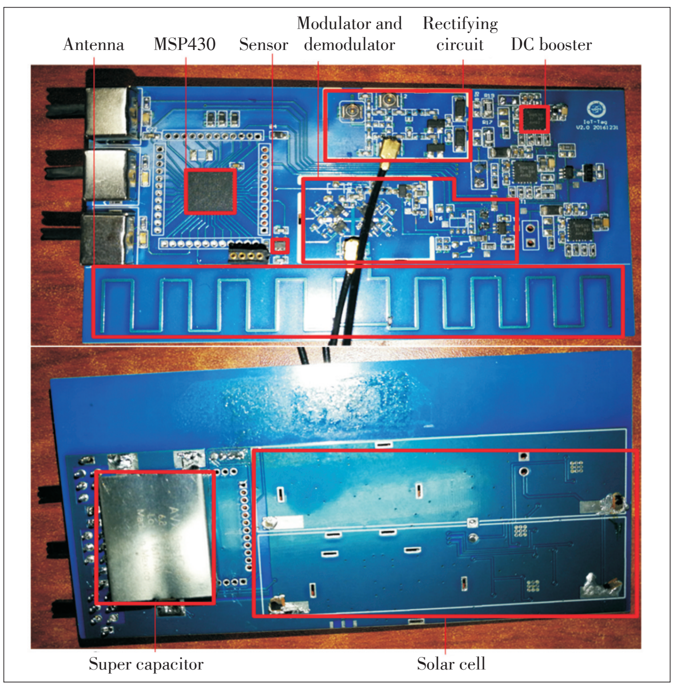

▲Figure 6. The circuit board of the WSN tag.

a step of 5°C. The test environment of WSN tag temperature is shown in **Fig. 7**. A self-designed UHF RFID reader was used for custom sensing command.

Fig. 8 compares the real temperature and test temperature. The horizontal axis represents N_{ADC} produced by the ADC, the vertical axis represents the temperature. We use the inverse transform of generating a N_{ADC} value to calculate the ambient temperature according to (1) and (2). From this figure, the test temperature is basically consistent with the real temperature.

4.3 Testing of Tag Protocol Performance

The distance within which the R420 reader can inventory the WSN tag successfully can be calculated by the friss electromagnetic wave propagation formula. The antennas of the reader and tag were placed on stands 2.4 m above the floor. The sensitivity of R420 reader is -82 dBm. The power transmitted is 30 dBm by the R420 reader, and the line loss L_{loss} is 1 dB. The gain of transmit antenna G_1 is 9 dBi, and the gain of tag antenna G_2 is 1 dBi. The sensitivity of tag, P_e, is −32 dBm, and the operating frequency is 920 MHz. The two antennas are both circular polarization, so the polarization loss, G_3, is 0 dB. The loss of the backscatter, G_4, is −6 dB. The distance within which the WSN tag can receive the available signal from the reader can be calculated by the following Friss equation:

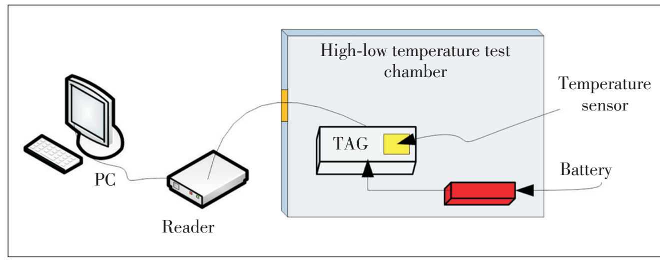

▲Figure 7. The test environment of WSN tag temperature.

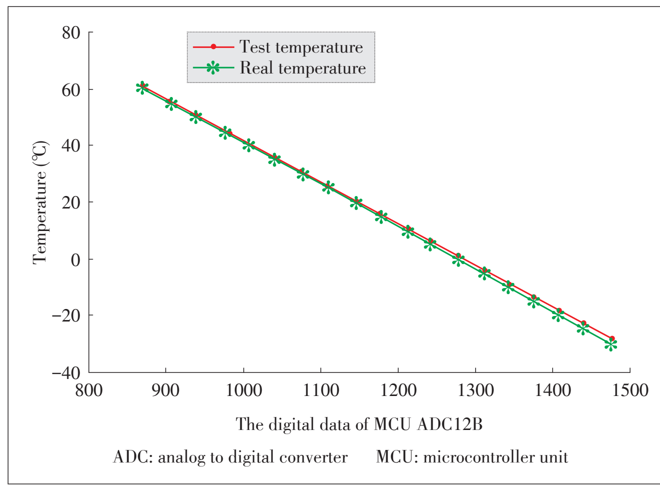

▲Figure 8. The contrast of test temperature and real temperature.

$$P_e = P_1 - L_{loss} + G_1 + G_2 + G_3 + 10\lg\left(\frac{\lambda}{4\pi r_1}\right)^2. \qquad (4)$$

Therefore, r_1 = 116 m. Similarly, by the Friss equation, P_3 is the power reader received from the backscatter of the WSN tag. Accordingly, it is possible to calculate the distance r_2 within which the reader can receive available reply signals by (5).

$$P_3 = P_1 - 2L_{loss} + G_4 + 2(G_1 + G_2 + G_3) + 10\lg\left(\frac{\lambda}{4\pi r_2}\right)^4. \qquad (5)$$

Therefore, r_2 = 32.68 m. **Table 4** shows the test distances in various modes of the reader, and some test distances are obviously beyond the theoretical distances, which are due to the influence of multipath effects.

5 Conclusions

The wireless energy-harvested WSN tag has been developed

▼Table 4. Test distances in various modes

Reader mode	R->T (kbit/s)	T->R (kbit/s)	r_2 (m)	r_1 (m)
Autoset dense reader	≈70	≈426.66	19	91.2
Autoset static	≈70	≈426.66	20	93.8
Max throughput	≈70	≈426.66	23	90.9
Hybrid mode	≈70	≈426.66	27	94.9
Dense reader M=4(1)	≈50	≈320	33	96.4
Dense reader M=4(2)	≈70	≈320	35.2	96.4
Dense reader M=8	≈70	≈320	36.5	97.4

in circuit board (Fig. 6). Reducing power and obtaining renewable energy are main advantages of the WSN tag. This paper presents the relevant wireless energy harvesting, common tag protocol, miller coding, extended miller coding and sensing functions. The test results of energy harvesting are consistent with the theoretical values. The rectifier efficiency reaches 39% when the rectifier circuit has input of -14 dbm and output voltage of 360 mV that is greater than 330 mV, which meets the condition of the DC Booster circuit cold start. The WSN tag successfully implements the common ISO/IEC 18000-6C protocol standard, and the sensitivity of the WSN tag is up to -32 dBm. The WSN tag also implements low speed mode for saving power. The extensional miller coding has first been implemented in the assembler. In the future, we plan to design multi-band RF energy harvesting system, to implement more applications of the WSN tag for the cellular IoT.

References

[1] S. T. Hsieh, "RFID medical information system: a system implementation on MSP430 platform," in *International Conference on Consumer Electronics, Communications and Networks (CECNet)*, Xian Ning, China, 2011, pp. 1-4. doi: 10.1109/CECNET.2011.5768332.
[2] Y. S. Lin, Z. Y. Guo, Y. S. Huang, and C. H. Yeh, "A low-power UHF passive RFID transponder chip in 0.18 μm CMOS," in *IEEE Wireless Power Transfer Conference (WPTC)*, Taipei, China, 2017, pp. 1-5. doi:10.1109/WPT.2017.7953802.
[3] H. Reinisch, M. W. flecker, S. Gruber, et al., "A multifrequency passive sensing tag with on-chip temperature sensor and off-chip sensor interface using EPC HF and UHF RFID technology," *IEEE Journal of Solid-State Circuits*, vol. 46, no. 12, pp. 3075-3088, Dec. 2011. doi: 10.1109/JSSC.2011.2167548.
[4] S. Q. Geng, L. G. Hou, J. H. Wang, et al., "Design of RFID active tag system based on MSP430," *IET 2nd International Conference on Wireless, Mobile and Multimedia Networks (ICWMMN 2008)*, Beijing, China, 2008, pp. 139-142. doi: 10.1049/cp:20080956.
[5] T. Skaik, "A quad-band rectifier design with improved matching bandwidth for RF energy harvesting applications," in *International Conference on Promising Electronic Technologies (ICPET)*, Deir El-Balah, Palestine, 2017, pp. 82-86. doi: 10.1109/ICPET.2017.21.
[6] X. Li, J. Wang, X. Wu, and H. Zhao, "A dual-band integrated wireless energy harvesting system," in *2017 International Applied Computational Electromagnetics Society Symposium (ACES)*, Suzhou, China, 2017, pp. 1-2.
[7] A. Mouapi, N. Hakem, and N. Kandil, "High efficiency rectifier for RF energy harvesting in the GSM band," in *2017 IEEE International Symposium on Antennas and Propagation & USNC/URSI National Radio Science Meeting*, San Diego, USA, 2017, pp. 1617-1618. doi: 10.1109/APUSNCURSINRSM.2017.8072851.
[8] P. Mhatre, R. Duche, S. Nawale, and P. Patil, "RF power harvesting system for RFID applications in multiband systems," in *6th International Conference on Computing, Communication and Networking Technologies (ICCCNT)*, Denton, USA, 2015, pp. 1-5. doi: 10.1109/ICCCNT.2015.7395226.
[9] S. Jung, D. Y. H. Chun, W. Kim, et al., "UWB sensor chip measurement system implementation using labview and MCU board," in *ICTC 2011*, Seoul, Korea, 2011, pp. 649-651. doi: 10.1109/ICTC.2011.6082679.
[10] Q. Zhang, T. Lin, and J. Yang, "The acquisition and analysis of vibration energy signal generated by magnetic shape memory alloys," in *29th Chinese Control and Decision Conference (CCDC)*, Chongqing, China, 2017, pp. 7019-7022. doi: 10.1109/CCDC.2017.7978447.
[11] C. Boyer and S. Roy, "Backscatter communication and RFID: coding, energy, and MIMO analysis," *IEEE Transactions on Communications*, vol. 62, no. 3, pp. 770-785, Mar. 2014. doi: 10.1109/TCOMM.2013.120713.130417.
[12] A. Sample, D. Yeager, P. Powledge, and J. Smith, "Design of a passively powered, programmable sensing platform for UHF RFID systems," in *Proc. 2007 IEEE International Conference on RFID*, Grapevine, USA, 2007, pp. 149-156. doi: 10.1109/RFID.2007.346163.
[13] M. A. Khan, M. Sharma, and R. B. Prabhu, "FSM based FM0 and Miller encoder for UHF RFID tag emulator," in *IEEE International Advance Computing Conference.*, Patiala, India, 2009, pp. 1317-1322. doi: 10.1109/IADCC.2009.4809207.

Manuscript received: 2017-09-07

Biographies

LI Gang (ligang1986718@163.com) received his M.E. degree from Chengdu University of Technology, China in 2012. He has five years of research in communication integrated circuits. He has currently been pursuing his Ph.D. degree at School of Communication and Information Engineering, University of Electronic Science and Technology of China (UESTC), China since 2016. His research interests include RFID, wireless communication networks, cognitive radio networks, and information security.

XU Rui (xurui_uestc@163.com) is currently pursuing his master's degree at School of Communication and Information Engineering, UESTC, China. His research interests include programmed algorithm and embedded system, and RFID and IoT.

LI Zhenbing (thomaslizhenbing@163.com) is currently pursuing his Ph.D. degree at School of Communication and Information Engineering, UESTC, China. His research interests include RFID and IoT, and RF circuit and system.

ZHOU Jie (jie.zhou1994@hotmail.com) is currently pursuing his master's degree at School of Communication and Information Engineering, UESTC, China. His research interests include RFID and IoT, and RF circuit and system.

LI Jian (uestclijian@163.com) is an associate research fellow at School of Communication and Information Engineering, UESTC, China. His research interests include RFID, IoT, wireless communication systems and networks, and RF circuit and system.

WEN Guangjun (wgj@uestc.edu.cn) received his B.Sc. and the M. E. degrees from Chongqing University, China in 1986 and 1992, respectively, and his Ph.D. degree from UESTC, China in 1998. From July 1986 to February 1995, he was with Chongqing University as a lecturer. He was with UESTC from July 1998 to May 2000, and then with Electronics and Telecommunication Research Institute, Korea from May 2000 to May 2001, as a postdoctoral fellow. He was with Nanyang Technological University, Singapore, as a research fellow from May 2001 to September 2002. He worked for VS Electronic Pte Ltd (Singapore) and Sumitomo Electric Group (Yokohama, Japan) as a senior RF design engineer from September 2002 to August 2005. Since January 2004, he has been a professor with UESTC. His research interests include radio frequency integrated circuits and systems for various wireless communication systems, analysis and design of RFID tag and reader, circuit components and antennas design for the internet of things. He has authored or co-authored more than 200 journal papers and presented more than 120 conference papers.